

Microcontroller design for active vibration control

Antonio Zippo^{1,2, a*}, Francesco Pellicano^{1,2, b}, Giovanni Iarriccio^{1, c}

¹ University of Modena and Reggio Emilia - DIEF, 41121 Modena, Italy

² InterMech MoRe Centre, 41121 Modena, Italy

^aantonio.zippo@unimore.it, ^bfrancesco.pellicano@unimore.it, ^cgiovanni.iarriccio@unimore.it

Keywords: Active Vibration Control, Positive Position Feedback, Experiments

Abstract. Active Vibration Control (AVC) problem is successfully studied considering all the characteristics of a control problem. The controlled system consists of a honeycomb panel of carbon fiber. Expensive devices are in general used for setting up and designing AVC this due to limitations for practical implementation. In our work we point to a low cost and practical solution using a microcontroller that has been verified. The honeycomb plate has been forced with out of plane load using an electrodynamic shaker at resonances that has been identified by experimental modal analysis. Piezoceramic patches are used as sensor and actuator for the control. Multiple analog signal processing circuits were developed to scale and shift the signal at the input and output of the MCU. The Positive Position Feedback (PPF) control algorithm is proposed, and a campaign of tests are carried out with harmonic excitations at resonance frequencies. Experimental results show an amplitude velocity reduction from 50% to 77% less and Power Spectral Density (PSD) attenuation up to 12.8 dB. The size and structural properties of the MFC patches, the control unit and structure under control are suitable for automobile and aerospace applications.

Introduction

In the last years, more and more Active Vibration Control has been increasing a lot of consideration, problem related to uncontrolled vibrations finds its application in wide range of industries, as for example: body plates of automobiles, preventing the bending of aerodynamic components in motorsports or reducing unwanted noise and resonance response; also in the aerospace sector, active vibration control finds its application as in [1] where Ye-Lin Lee describe a reduction of vibration up to 98% in simulations of a lift-offset compound helicopter using two active control techniques. Moreover, studies regarding experimental activities and problems of complex systems, as in [2], [3] and [4] demonstrate the importance of experimental investigations.

Different techniques and algorithms can be used to control the vibration of a structure as the author in [5] devised an energy-fuzzy adaptive PD control to stabilize the structures in subsonic and transonic regime, or as in [6], Balakrishna used piezoceramic actuation embedded to the structure to reduce the response, producing a practical solution for the sting vibration. Another method is explained in [7] where Oveisi and Nestorović used a frequency domain subspace identification for robust control design, or in [8] Electrically Controlled Rotor (ECR) has been controlled developing a Kalman filter-based control algorithm.

Example of microcontroller for active vibration control applications are present as in [9] using an Arduino Uno, with clock speed of 16 MHz.

In [10], Moon K.Kwak developed a MIMO PPF controller realized by a dSpace DSP board, with the sampling frequency of ADC and DAC being 50 kHz, A.Zippo et al., in [11], showed experiments implementing a variety of configurations: SISO, multiSISO and MIMO on a free-free composite panel with PPF method and MFC patches both for sensors and actuators in linear and nonlinear range. Moreover, analytically define chaotic structures is stimulating for improving

our knowledge in the occurrence of vibrations related to complex systems [12] with quasiperiodic and chaotic motion [13].

In [14], Isabelle Bruant et al., used genetic algorithm for optimal placing patches for ACV.

Experimental modal analysis

In figure 1 is shown the experimental setup, while in figure 2 the TestLab sum of FRF is shown, this graph help to experimental identify modes of vibration.

Eleven modes have been identified in total and in figure 3 and 4 are represented the reconstructed modal shapes at 25.13Hz and at 132.31Hz, the respective identified damping is 0.33% and 0.18%



Figure 1. Experimental modal analysis setup

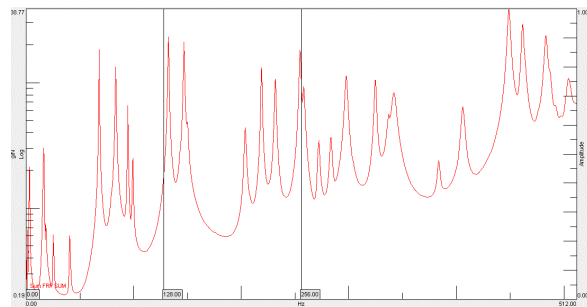


Figure 2: Sum of FRFs of the plate

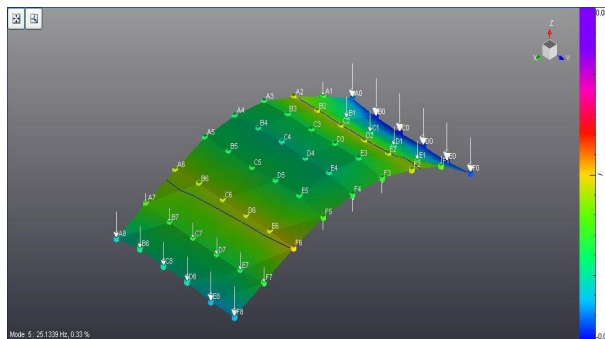


Figure 3: 2nd mode of vibration at 25.13 Hz

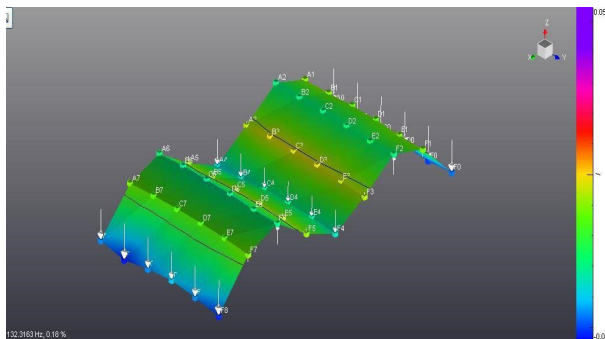


Figure 4: Vibration mode at 132.31 Hz

Sensor and actuator selection

In Table 1 are presented the selected. MFC patches used as sensor and actuator, the Macro Fiber Composites (MFC) can be used both as sensor or actuator, depending on the voltage is measured or powered from or to the patch, they consist of piezo-ceramic rods sandwiched in a design of multi-layers of electrodes and polyimide film. In figure 5 their location on the plate is showed. The physical effect used by this materials is the d33, achieved by the stack arrangement of the piezoelectric material, that are configured so that when a voltage is applied across the electrodes, the stack expands in length (commonly considered as 3-3 axis) and for a certain voltage, the net static displacement δ of the piezoelectric ceramic actuator is:

$$\delta = \frac{d_{33}V + \frac{F}{K_a}}{1 + \frac{K}{K_a}} \tag{1}$$

where d_{33} is the strain constant of the piezoelectric material in the 3-3 axis, K is the external spring stiffness, K_a is the actuator stiffness ($K_a = E_a A_a / L_a$, where E_a , A_a , and L_a are the actuator's young's modulus, cross-sectional area, and length, respectively). F is the external load force.

Table 1. Dimensions and electrical properties of MFC patches

	M8507-P1 (sensor)	M8557-P1 (actuator)
Active length [mm]	85	85
Active width [mm]	7	57
Overall length [mm]	101	103
Overall width [mm]	13	64
Capacitance [nF]	3.1	16
Free strain [ppm]	1035	1350
Blocking force [N]	65	693

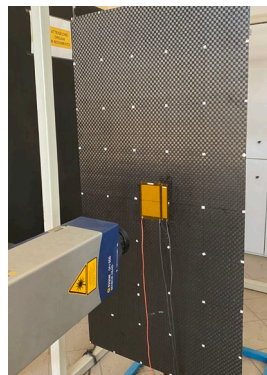


Figure 5: patches location

Micro controller unit selection

The application of AVC in certain industrial application as automotive adds more constraints for the implementation as compact and light weight. Indeed, a 32-bit Micro Controller Unit (MCU) from Texas Instrument is used for the study and experiment performing on a composite sandwich plate the control.

The C2000 32-bit microcontrollers are optimized for processing, sensing and actuation to improve closed-loop performance in real time.

The main feature are:

- 32-bit C28x architecture floating point MCU
- 200 MHz processing speed
- Selectable 16-bit & 12-bit SAR ADC, up to 14 MSPS system throughput
- 1MB flash & 204KB RAM
- USB communication with Simulink interface

Analog circuits design

The analog signal processing circuits are needed to scale and shift the signal at output of the sensors and MCU to match the input of the signal requirement at the succeeding element to improve resolution, hence the performance and avoid signal saturation. In figure 6 is showed the electric scheme of the system.

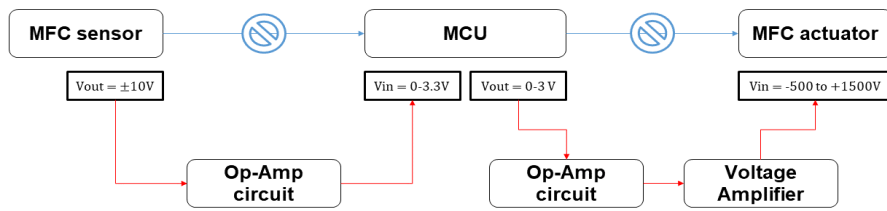


Figure 6: Electric schemes

The circuits are first prototyped in a breadboard, and after the components are implemented to a PCB to make it more compact and lightweight. BNC connectors has been used at the signal input and output for all the boards.

In the manufacture of the signal processing circuits, few of the resistors were replaced by trimmers to add the flexibility of tuning the gain and bias which can account for any errors during assembly and soldering.

Control algorithm

The PPF controller is a filter of second order that tends to maximize damping in the frequency specified without destabilizing other modes, and thus reducing spillover. PPF controller is modelled as a second-order dynamic system, which is represented by the following equation,

$$\ddot{\eta}(t) + 2\zeta_c\omega_c\dot{\eta}(t) + \omega_c^2\eta(t) = kq\omega_c^2 \quad (2)$$

Where ζ_c is the damping ratio of the compensator, ω_c is the frequency of the compensator and k is the compensator gain. The transfer function takes the form:

$$H(s) = \frac{\omega_c^2}{s^2 + 2\zeta_c\omega_c s + \omega_c^2} \quad (3)$$

At frequencies above ω_c the slope of the transfer function amplitude is negative and very steep (-40 dB/octave), so it reduces the problem of spillover for vibrations at higher frequencies. On the contrary, at frequencies below ω_c the bode diagram of $H(s)$ has an amplitude of 0 dB, the simulink model is showed in figure 7.

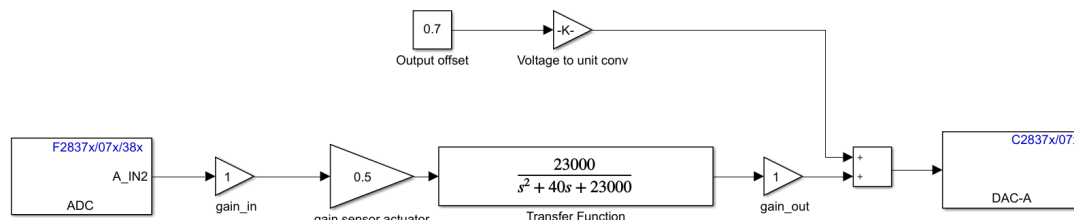


Figure 7. PPF controller modelled in simulink

Setup and results

The plate is excited using a traditional electrodynamic shaker, placed behind the plate. The force applied by the shaker is measured by a dynamic force transducer and the PPF algorithm is compiled and uploaded in the flash of MCU. The actuator and sensor are placed to interact optimally with the selected modes.

Results of the second vibration mode control at 25.17Hz are a Velocity reduction of 74.18%, a PSD amplitude attenuation of 11.76 dB inn a Settling time of about 1 second, in figure 8 is shown respectively the time history and PSD of the shaker input signal, and the PSD of the control, while in figure 9 is presented the time history while the control is activated.

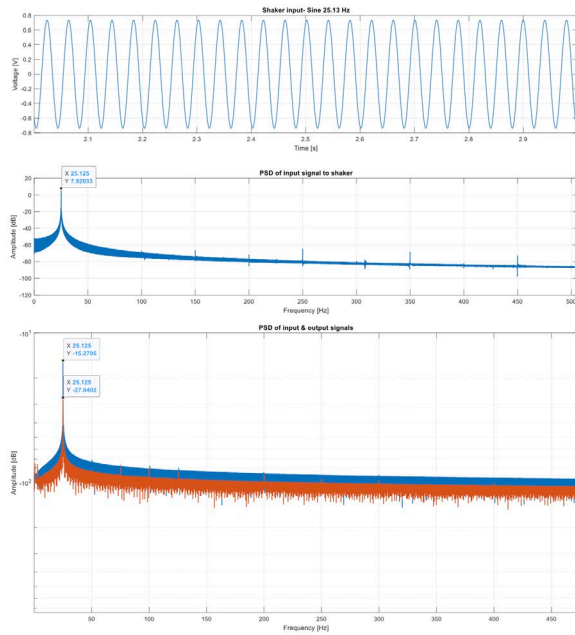


Figure 8: PPF controller modelled in simulink

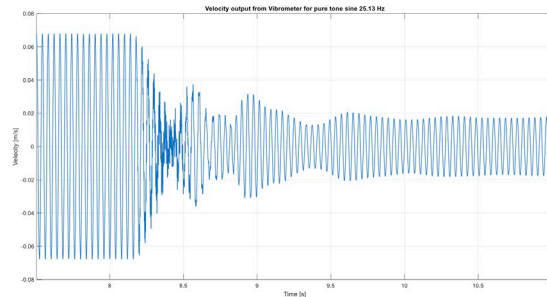


Figure 9: TH during control activation

Conclusions

This investigation designed an Active Vibration Control System on the base of a C2000 32-bit microcontroller unit by means of MFC patches used for sensing the disturbances and actuate a controlling force by means of a second order filter algorithm (Positive Position Feedback method). This work shows more practical solution can be implemented also with low-cost central unit and allow a direct implementation in automotive industrial problems. The control techniques discussed, and the developed hardware was proved effective in suppressing the amplitude of vibration when subjected to harmonic excitations. Nevertheless, harmonic disturbances are not common, forcing alone a system in a practical application, further studies will be carry out applying to the panel random excitations and complex signals to better reproducing and testing real case studies.

References

- [1] Ye-Lin Lee, Do-Hyung Kim, Jae-Sang Park, Sung-Boo Hong. Vibration reduction simulations of a lift-offset compound helicopter using two active control techniques. *Aerospace Science and Technology* 2020; 106181. <https://doi.org/10.1016/j.ast.2020.106181>
- [2] Zippo A., Iarriccio G., Pellicano F., Shmatko T., Vibrations of plates with complex shape: Experimental modal analysis, finite element method, and R-functions method, (2020) *Shock and Vibration*, 2020. <https://doi.org/10.1155/2020/8882867>
- [3] Iarriccio G., Zippo A., Pellicano F., Barbieri M., Resonances and nonlinear vibrations of circular cylindrical shells, effects of thermal gradients, (2021) *Proceedings of the Institution of Mechanical Engineers, Part C: Journal of Mechanical Engineering Science*, 235 (20), pp. 4818 – 4832. <https://doi.org/10.1177/0954406220907616>
- [4] Pellicano F., Zippo A., Iarriccio G., Barbieri M., Experimental Study on Nonlinear Random Excitation, (2020) *Lecture Notes in Mechanical Engineering*, pp. 637 – 648. https://doi.org/10.1007/978-3-030-31154-4_54
- [5] Wei LIU, Weixiao LIU, Mengde ZHOU, Linlin TANG, Qinqin WANG, Zhengquan WEN, Zhuang YAO, Xiaojing YUAN. An active vibration control method based on energy-fuzzy for

- cantilever structures excited by aerodynamic loads. Chinese Journal of Aeronautics, Volume 34, Issue 9, 2021; 1000-9361. <https://doi.org/10.1016/j.cja.2020.07.001>
- [6] Balakrishna, Sundareswara & Houlden, Heather & Butler, David & White, Richard. Development of a Wind Tunnel Active Vibration Reduction System. 2007; 10.2514/6.2007-961. <https://doi.org/10.2514/6.2007-961>
- [7] Atta Oveisi, Tamara Nestorović, Allahyar Montazeri. Frequency Domain Subspace Identification of Multivariable Dynamical Systems for Robust Control Design. IFAC, Volume 51, Issue 15, 2018; 2405-8963. <https://doi.org/10.1016/j.ifacol.2018.09.065>
- [8] Jinchao MA, Yang LU, Taoyong SU, Shujun GUAN. Experimental research of active vibration and noise control of electrically controlled rotor. Chinese Journal of Aeronautics, Volume 34, Issue 11. 2021; 1000-9361. <https://doi.org/10.1016/j.cja.2020.10.027>
- [9] Wang, Z, & Keogh, P. Active vibration control for robotic machining. Proceedings of the ASME 2017 International Mechanical Engineering Congress and Exposition. Volume 2: Advanced Manufacturing. Tampa, Florida, USA. November 3–9, 2017. V002T02A079. ASME. <https://doi.org/10.1115/IMECE2017-71670>
- [10] Moon K. Kwak, Seok Heo. Active vibration control of smart grid structure by multi- input and multioutput positive position feedback controller. Journal of Sound and Vibration, Volume 304, Issues 1–2, 2007. <https://doi.org/10.1016/j.jsv.2007.02.021>
- [11] Zippo, Antonio & Ferrari, Giovanni & Amabili, Marco & Barbieri, Marco & Pellicano, Francesco. Active vibration control of a composite sandwich plate. Composite Structures. 2015. 128. <https://doi.org/10.1016/j.compstruct.2015.03.037>
- [12] Hemmatnezhad M., Iarriccio G., Zippo A., Pellicano F., Modal localization in vibrations of circular cylindrical shells with geometric imperfections (2022) Thin-Walled Structures, 181, art. no. 110079. <https://doi.org/10.1016/j.tws.2022.110079>
- [13] Iarriccio G., Zippo A., Pellicano F., Asymmetric vibrations and chaos in spherical caps under uniform time-varying pressure fields, (2022) Nonlinear Dynamics, 107 (1), pp. 313 – 329. <https://doi.org/10.1007/s11071-021-07033-7>
- [14] Isabelle Bruant, Laurent Gallimard, Shahram Nikoukar. Optimal piezoelectric actuator and sensor location for active vibration control, using genetic algorithm. Journal of Sound and Vibration, Volume 329, Issue 10, 2010. <https://doi.org/10.1016/j.jsv.2009.12.001>